

Energy and current correlations in mesoscopic rings and quantum dots

Yuval Gefen

Department of Physics, The Weizmann Institute of Science, Rehovot, 76100 Israel

Bertrand Reulet and Hélène Bouchiat

Laboratoire de Physique des Solides, Bâtiment 510, Université Paris-Sud, 91405 Orsay, France

(Received 5 August 1992)

With a view to some of the late developments in the thermodynamics of mesoscopic systems, we examine the problem of level correlations in moderately disordered (diffusive) conductors. We briefly review the thermodynamic relations, employed within perturbation theory. We calculate correlation functions among single electron levels, and magnetic-field (magnetic-flux) derivatives thereof. Specifically, we evaluate both single-level current and single-level curvature correlations, and use them to examine the typical current, the paramagnetic susceptibility, and the energy “power spectrum” of Aharonov-Bohm geometries, derived previously. We stress the role of spectral rigidity, and present comparison with simply connected systems subject to a magnetic field.

I. INTRODUCTION

Isolated mesoscopic systems are characterized by their single-electron-level spectra and their related eigenstates. In the absence of electron-electron interactions, the spectra of the specific realizations forming a statistical ensemble determine many of the physical properties, including thermodynamical quantities.

Commonly, one is concerned with identifying and calculating (or measuring) quantities that characterize the entire ensemble rather than studying a particular member of the ensemble. In this context, the recent observation of persistent currents¹⁻⁴ in isolated mesoscopic rings⁵ threaded by magnetic flux are particularly important. These currents are calculated by taking the flux derivative of the total free energy. Within the independent-electron picture they can be computed (excluding spin), given the flux dependence of each energy level.

In a seminal work, Altshuler and Shklovskii⁶ have identified two important energies, namely the average level spacing (excluding spin) Δ , and the Thouless energy $E_c = \hbar D / L^2$ (D being the diffusivity, L the relevant linear system's size) as relevant scales in the spectral correlations. In particular they have calculated the fluctuation in the number of levels within an energy window ΔE , and showed that the results of random matrix theory hold for energy scales between Δ and E_c , while different types of correlations are to be found on scales larger than E_c (but smaller than the inverse elastic mean-free time). The introduction of magnetic field (or magnetic flux) tends to make the spectrum more rigid.

In the present work we focus on a somewhat different quantity, namely the correlations among flux derivatives of single electron levels. The motivation for this study is outlined below. We show that the (ensemble-averaged) flux-dependent part of these correlations exhibits rigidity, for $\Delta E > E_c$, much larger than the flux-independent part. This provides an explanation for the rigidity (on large energy scales) of such quantities as the typical current.

The outline of the present paper is as follows. In Sec. II we provide further motivation for calculating the single level correlation functions. We also review certain relations, originally derived by Imry,⁷ for flux-dependent correlations in the density of states. The typical current and the energy “power spectrum” of the single-level currents in a cylindrical geometry are discussed in Sec. III. Correlations of single-level curvatures are studied in Sec. IV for a cylindrical geometry, and are contrasted with those of a singly connected geometry. Conclusions and some caveats concerning our analysis are presented in Sec. V.

II. FLUX-DEPENDENT CORRELATIONS IN THE DENSITY OF STATES: MAINLY A REVIEW

A. Motivation

For our present analysis we shall need to calculate correlation functions between single electron energy levels at various values of the magnetic flux, and derivatives thereof. The reason for doing so lies in three rather remarkable results that have been obtained over the past few years.

1. Typical current

Single electron energy levels of an Aharonov-Bohm cylinder (ring) are magnetic flux sensitive. Denoting the Aharonov-Bohm flux threading the ring by ϕ , the n th single electron energy $\varepsilon_n(\phi)$ is a periodic function of ϕ with a period $\phi_0 = h/e$. The latter is often referred to as a flux quantum. The (persistent) current carried by the n th level,

$$i_n(\phi) = - \frac{\partial \varepsilon_n(\phi)}{\partial \phi}, \quad (2.1)$$

measures the sensitivity of this level to variations in the

flux. These, by an appropriate gauge transformation, may be related to changes in boundary conditions. At zero temperature, the *total* current is given by summing up all single-level current contributions up to the Fermi energy ε_F :

$$I = \sum_{\varepsilon_n \leq \varepsilon_F} i_n . \quad (2.2)$$

There are numerical indications that I is a random Gaussian variable.³ The average current is given by ensemble averaging I . At the same time, one may calculate the *typical* current. Defining the energy window ΔE as the interval $[\varepsilon_F - \Delta E, \varepsilon_F]$, one may evaluate the typical current $I_{\Delta E}^{\text{typ}}$ within this energy window:

$$I_{\Delta E}^{\text{typ}} \equiv \left\langle \left[\sum_{\varepsilon_n \in [\varepsilon_F - \Delta E, \varepsilon_F]} i_n \right]^2 \right\rangle^{1/2} , \quad (2.3)$$

where $\langle \rangle$ denotes ensemble averaging.

It has been found^{8,9} that the typical current of a short two-dimensional cylinder is

$$\begin{aligned} &\sim \sqrt{\Delta E / \Delta} \frac{e \Delta}{\hbar} , \quad \Delta \ll \Delta E \ll E_c , \\ &\sim \sqrt{E_c / \Delta} \frac{e \Delta}{\hbar} , \quad \hbar / \tau \gg \Delta E \gg E_c , \end{aligned} \quad (2.4)$$

where τ is the elastic mean free time. Equation (2.4) implies that the typical current increases with the number of levels within the energy window, reaching saturation as this number becomes equal to the effective number of transverse channels, $M_{\text{eff}} \approx E_c / \Delta \sim M(l/L)$, (M being the number of occupied transverse modes and l the elastic mean free path).

Inspection of Eq. (2.3) reveals that the expression for the typical current includes a summation over pairs of single-level currents, $\langle i_n i_m \rangle$. The fact that the sum in Eq. (2.3) saturates at $\Delta E \approx E_c$ suggests strong correlations that suppress the contribution of such current pairs for $|\varepsilon_n - \varepsilon_m| \gg E_c$. An explicit derivation of this behavior relying on a study of the energy spectrum is, evidently, called for.

2. Enhanced orbital paramagnetism

In several recent works it has been argued that the magnetic susceptibility of canonically averaged rings (near $\phi=0$), arising from orbital contributions, is paramagnetic in nature.¹⁰⁻¹⁹ The term ‘‘canonical’’ here implies that the number of electrons within each ensemble member is held flux independent. Similarly, simply connected systems (quantum dots) may exhibit large orbital paramagnetic susceptibility at weak magnetic fields.^{15,20,21}

One appealing argument, due to Bouchiat and Montambaux,^{11,12} explaining this effect, assumes that single electron levels at, e.g., zero field, occasionally appear in pairs which are close in energy. These levels now tend to repel each other as the magnetic flux is turned on (this is, for example, a direct consequence of second-order perturbation theory). This results in the levels having rather large curvatures of opposite signs (the lower level of the

pair is negatively curved, while the upper one is curved upwards). Now, at zero temperature, each level is either empty or occupied. When both levels are occupied (i.e., below the Fermi energy), their contribution to the total susceptibility is small, as the respective contributions of each level nearly cancel. (Evidently, when both levels are empty, their contribution is zero.) If only one (the lower) is occupied, the total contribution of this pair will give rise to a large term of a paramagnetic sign. This picture, evident in the limit of very weak disorder, is less trivial when the amount of disorder is significant. It is desirable to confirm the above picture, based on analysis of the spectrum, and to demonstrate that consecutive levels indeed tend to be anticorrelated in curvature.

3. Power spectrum of single-level currents

This point is somewhat technical and not so much related to an experiment as the two topics mentioned above. In a recent study by Bouchiat, Montambaux, and Sigeti,¹³ various aspects of a ring’s spectrum were investigated, combining numerical computations with scaling arguments. Defining

$$\varepsilon_n(\phi) = \sum_{m=0}^{\infty} \lambda_m(n) \cos(2\pi m \phi / \phi_0) , \quad (2.5)$$

they have considered the Fourier transform

$$\lambda_m(n) = \int_{f_{\min}}^1 b_m(f) e^{i2\pi f n} df , \quad (2.6)$$

where f_{\min} is of the order of Δ / ε_F . The power spectrum is defined as

$$B_m(f) = \langle b_m(f)^2 \rangle . \quad (2.7)$$

Bouchiat, Montambaux, and Sigeti have found that the ‘‘power spectrum’’ $B_m(f)$ presents a sharp cutoff $f_m \sim m^2 \Delta / 2\pi E_c$, below which $B_m(f) \sim 0$. On the other hand, for $f \gg f_m$, $B_m(f)$ decays like a power law. In particular, it was found for the power spectrum $B(f) \equiv \Delta \varepsilon_n \equiv \varepsilon_n(\phi / \phi_0 = 0) - \varepsilon_n(\phi / \phi_0 = \frac{1}{2})$ varies as

$$B(f) \sim \frac{1}{f} \quad (2.8)$$

for frequencies $f \gg \Delta / E_c$. It is our purpose here to derive analytically $B_m(f)$ and $B(f)$ from our spectral analysis.

B. The basic formalism: A terse review

Our analysis here is heavily based on a formulation developed by Altshuler and Shklovskii⁶ to study fluctuations in mesoscopic systems. Later works^{8,14-22} have relied on this seminal work. Some results of our analysis have already appeared in recent papers.^{9,19-22}

Let us define the density of states (as function of energy ε and flux ϕ) by $n(\varepsilon, \phi)$. Imry’s starting point⁷ was to observe that the total number of electrons (at zero temperature) was given by

$$\int_0^{\mu_N(\phi)} n(\varepsilon, \phi) d\varepsilon = N , \quad (2.9)$$

where $\mu_N(\phi)$ is the flux-dependent chemical potential (at zero temperature) corresponding to a flux-independent number of electrons. In other words, $\mu_N(\phi)$ is defined to be the energy half way between the N th and the $N+1$ st level: this sample specific quantity may be written as

$$\mu_N(\phi) = \bar{\mu}_N + \delta\mu_N(\phi), \quad (2.10)$$

where the overbar denotes averaging over flux. Invoking the impurity averaging notation $\langle \rangle$, we may write

$$\begin{aligned} \mu_N(\phi) &= \langle \bar{\mu}_N \rangle + \bar{\mu}_N - \langle \bar{\mu}_N \rangle + \delta\mu_N(\phi) \\ &\equiv \langle \bar{\mu}_N \rangle + \delta\bar{\mu}_N + \delta\mu_N(\phi), \end{aligned} \quad (2.11)$$

with $\delta\bar{\mu}_N = \bar{\mu}_N - \langle \bar{\mu}_N \rangle$. One may also write

$$n(\varepsilon, \phi) = \langle n(\varepsilon, \phi) \rangle + \delta n(\varepsilon, \phi), \quad (2.12)$$

and define

$$\delta N(E, \phi) \equiv \int_0^E \delta n(\varepsilon, \phi) d\varepsilon. \quad (2.13)$$

It can be shown that to leading order⁷

$$\delta N(\mu_N(\phi), \phi) + n_N^0 [\delta\bar{\mu}_N + \delta\mu_N(\phi)] \approx 0, \quad (2.14)$$

with

$$n_N^0 = n(\langle \bar{\mu}_N \rangle), \quad (2.15)$$

independent of the flux. It thus follows that

$$\begin{aligned} &\langle \delta N(\langle \bar{\mu}_N \rangle, \phi) \delta N(\langle \bar{\mu}_M \rangle, \phi') \rangle \\ &= n_N^0 n_M^0 \langle [\delta\bar{\mu}_N + \delta\mu_N(\phi)] [\delta\bar{\mu}_M + \delta\mu_M(\phi')] \rangle. \end{aligned} \quad (2.16)$$

We shall assume that, to leading order, and as long as $|N-M|$ is not too large, $n_N^0 \simeq n_M^0 \simeq n^0$. Moreover, the right-hand side (rhs) of Eq. (2.16) may be replaced at zero temperature, to leading order, by

$$(n^0)^2 \langle \varepsilon_N(\phi) \varepsilon_M(\phi') \rangle, \quad (2.17)$$

where $\varepsilon_N(\phi)$ denotes the (flux-dependent) N th energy level. Thus, by evaluating the left-hand side (lhs) of Eq. (2.16) we shall be able to obtain information concerning correlations among energy levels and their derivatives (currents, curvatures, etc.).

To this end we apply a zero-temperature Green's-

function technique, calculating contributions due to double cooperon and double diffuson diagrams.⁶ The cooperon term will depend on $\phi^+ = \phi_1 + \phi_2$, while the diffuson part on $\phi^- = \phi_2 - \phi_1$. Similarly we have inelastic rates γ^+ and γ^- , which, in our analysis, are taken to be equal to each other. In performing this analysis we recall some of the limitations of perturbation theory:

(i) $|\varepsilon_N - \varepsilon_M| \lesssim \hbar/\tau \ll \langle \bar{\mu}_N \rangle, \langle \bar{\mu}_M \rangle$. (When the first inequality breaks down, one may still employ perturbation theory, but the form of the correlators will change.²³)

(ii) As $|\varepsilon_N - \varepsilon_M|$ approaches Δ (the average level spacing), other diagrams become important, leading to the breakdown of this perturbation theory. On energy scales close to Δ , γ (if larger than Δ) takes over. We shall not discuss here the nonperturbative regime^{18,24} $\gamma < \Delta$.

(iii) For $\gamma \ll \Delta$ the theory breaks down, for $|\phi^+|, |\phi^-| \lesssim \phi_0 \sqrt{\Delta/E_c}$. But for $\gamma > \Delta$ one is allowed to consider this ‘‘superweak’’ regime of the flux within perturbation theory.

The correlation function of the fluctuations in particle numbers is given in terms of the cooperon and diffuson contributions:

$$\begin{aligned} &\langle \delta N(\varepsilon_2, \phi_2) \delta N(\varepsilon_1, \phi_1) \rangle \\ &\equiv \int_{-\infty}^0 \int_{-\infty}^{-\delta} d\varepsilon_1 d\varepsilon_2 [K^C(\varepsilon_1, \phi_1; \varepsilon_2, \phi_2) \\ &\quad + K^D(\varepsilon_1, \phi_1; \varepsilon_2, \phi_2)]. \end{aligned} \quad (2.18)$$

Here we used the notation $\varepsilon_1 = N\Delta$, $\varepsilon_2 = M\Delta$, $\delta = \varepsilon_2 - \varepsilon_1$. Without loss of generality, we have set the Fermi energy at 0. We have approximated the bottom of the Fermi sea by $-\infty$, anticipating minor contributions from energy intervals beyond \hbar/τ .

The geometrical setup is depicted in Fig. 1. Periodic boundary conditions are imposed along the tangential direction, denoted as x , while fixed boundary conditions are imposed along the y and z directions. We thus use Cartesian coordinates to describe our large aspect ratio cylinder. L_x , L_y , and L_z are the respective perimeter, thickness, and length of the system.

We now expand the correlation function, Eq. (2.18), in a Fourier series, and find after some algebra (see, e.g., Refs. 14, 15, 20, and 25),

$$\langle \delta N(\varepsilon_2, \phi_2) \delta N(\varepsilon_1, \phi_1) \rangle - \langle \delta N(\varepsilon_2, 0) \delta N(\varepsilon_1, 0) \rangle \equiv \sum_{m=1}^{\infty} C_m \left[\cos 2\pi m \left(\frac{\phi_1 + \phi_2}{\phi_0} \right) + \cos 2\pi m \left(\frac{\phi_1 - \phi_2}{\phi_0} \right) \right]$$

with

$$C_m = \sum_{m=1}^{\infty} \frac{s^2}{\pi^2 m} \exp - \left\{ \left[\frac{\delta^2 + \gamma^2}{E_c^2} \right]^{1/4} \left[\cos \left[\frac{1}{2} \arctan \frac{\delta}{\gamma} \right] \right] m \right\} \cos \left\{ \left[\frac{\delta^2 + \gamma^2}{E_c^2} \right]^{1/4} \left[\sin \left[\frac{1}{2} \arctan \frac{\delta}{\gamma} \right] \right] m \right\}, \quad (2.19)$$

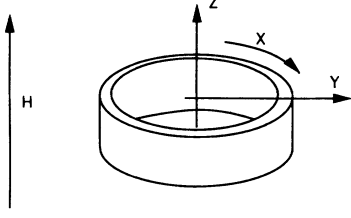


FIG. 1. Cylinder pierced by an Aharonov-Bohm flux.

where a flux-independent term (the zeroth harmonic) was subtracted from the correlation function. Here s is the spin degeneracy.

In the limit E_c , $\delta \gg \gamma \geq \Delta$ (implying $\arctg \delta/\gamma \approx \pi/2$), it is possible to write the correlation function of the m th harmonic as a function of the variable $m^2\delta/E_c$,

$$C_m = \frac{s^2}{\pi^2 m} F \left[m^2 \frac{\delta}{E_c} \right], \quad (2.20)$$

where

$$F(x) = \exp(-\sqrt{x/2}) \cos \sqrt{x/2}. \quad (2.21)$$

This asymptotic behavior contains information concerning correlations over energy scales larger than the level spacing. We shall use this result for our analysis of the typical total current.

Equations (2.20) and (2.21) imply that the number of effective harmonics contributing to the correlation function depends on the energy interval considered, δ . Within the present perturbation theory, δ exceeds the level spacing Δ . For $\delta \gtrsim \Delta$ the number of effective harmonics is $\sim \sqrt{E_c/\Delta} \sim \sqrt{g}$, where g is the dimensionless conductance.

III. TYPICAL CURRENT AND THE ENERGY POWER SPECTRUM OF SINGLE-LEVEL CURRENTS IN A CYLINDER

Equation (2.19) in conjunction with Eqs. (2.17) and (2.1) provides us also with the correlation function of the flux-dependent part of the energy levels as well as the correlations among single-level currents. At zero temperature the *total* current carried by a ring containing N electrons is given by summing up all the single-level contributions of the first N levels,

$$I(N, \phi) = \sum_{n=1}^N i_n(\phi). \quad (3.1)$$

The total typical value of $I(N, \phi)$ is given by

$$\langle I^2(N, \phi) \rangle = \sum_{n,p} \langle i_n i_p \rangle. \quad (3.2)$$

The total typical current is thus directly related to the correlations among the single-level currents. In the limit $N \gg 1$ we employ a quasicontinuous description of the spectrum, replacing Eq. (3.1) by [cf. Eq. (2.9)]

$$I(N, \phi) = \frac{1}{\Delta} \int_0^{\mu_N(\phi)} i(E, \phi) dE. \quad (3.3)$$

When evaluating *averaged* quantities it is essential to specify the type of statistical ensemble employed. For the square of the current, the distinction between canonical and grand canonical ensemble is not all that crucial, and $\mu_N(\phi)$ will be replaced by [cf. Eqs. (2.10) and (2.11)] $\langle \bar{\mu}_N \rangle \approx N\Delta$.

An alternative approach to relate the typical current to the single-level correlations is to express the former in terms of the “power spectrum” of the successive harmonics of the flux-dependent part of the energy levels [cf. (2.5) and (2.6)]

$$B_m(f) = \left\langle \left[\frac{1}{2\pi\Delta} \int_0^{\epsilon_F} \lambda_m(E) e^{2i\pi f(E/\Delta)} dE \right]^2 \right\rangle. \quad (3.4)$$

The rhs of Eq. (3.4) consists of the square of the ensemble-averaged Fourier transform of $\lambda_m(E)$, m denoting the m th harmonic in flux. Employing Eqs. (2.1), (2.5), and (2.6), we may write for the m th harmonics of the single-level current

$$\begin{aligned} \langle |i_m(E)|^2 \rangle &= \left\langle \left| \int_{\Delta/\epsilon_F}^1 \tilde{i}_m(f) e^{2i\pi f(E/\Delta)} df \right|^2 \right\rangle \\ &= \frac{4\pi^2 m^2}{\phi_0^2} \int_{\Delta/\epsilon_F}^1 B_m(f) df, \end{aligned} \quad (3.5)$$

and by Eq. (3.3)

$$\langle |\tilde{I}_m(f)|^2 \rangle = \frac{1}{4\pi^2 f^2} \langle |\tilde{i}_m(f)|^2 \rangle, \quad (3.6)$$

where we have used the fact that [cf. Eq. (2.6)]

$$\int df' \langle b_n(f) b_m(f') \rangle = \langle [b_m(f)]^2 \rangle \delta_{nm}. \quad (3.7)$$

Hence the power spectrum of the m th harmonic of the total current is

$$\langle |I_m(f)|^2 \rangle = \frac{m^2 B_m(f)}{f^2 \phi_0^2}. \quad (3.8)$$

Equations (3.5) and (3.6) demonstrate that the low-frequency behavior of $B_m(f)$, which controls the convergence of the integral of $B_m(f)/f^2$, is directly related to the large- N dependence of the typical current. More specifically, if $\lim_{f \rightarrow 0} B_m(f) \sim f^{1+x}$ with $x \leq 0$, then the m th harmonic of the total current $\lim_{N \gg 1} I_m$ (N electrons) $\sim N^{-x/2}$. On the other hand, if $x > 0$, the typical current for large N converges towards an N -independent limit. We next show that $B_m(f)$ vanishes, as $f \rightarrow 0$, faster than linearly. From Eqs. (2.1), (2.19), (3.4), and (3.7), it follows that

$$B_m(f) = \frac{\Delta}{4\pi^2} \int_{-\infty}^{+\infty} C_m(\delta) e^{2i\pi f(\delta/\Delta)} d\delta, \quad (3.9)$$

where the large-energy limit of $C_m(\delta)$ is given by Eqs. (2.20) and (2.21). Defining

$$f_m = \frac{\Delta m^2}{2\pi E_c}, \quad (3.10)$$

we obtain (for $f < \Delta/\gamma$)

$$B_m(f) = \frac{\Delta s^2}{2\pi^{3/2}} \frac{E_c}{m^3} \left(\frac{f_m}{f} \right)^{3/2} e^{-(f_m/f)}. \quad (3.11)$$

We have thus recovered, according to Ref. 13, that the energy power spectrum is nearly zero at small frequencies compared to f_m , goes through a maximum at a frequency close to f_m , and decays like a power law at high frequency; see Fig. 2. (The apparent disagreement between the numerical value of the exponent of this power law, $x = 1$, and the analytical one, $x = \frac{3}{2}$, is discussed below.) Using (3.8) and (3.9), the typical magnitude of the m th harmonic of the total current is calculated from

$$\langle I_m^2 \rangle = 4\pi^2 \int \langle I_m(f)^2 \rangle df, \quad (3.12)$$

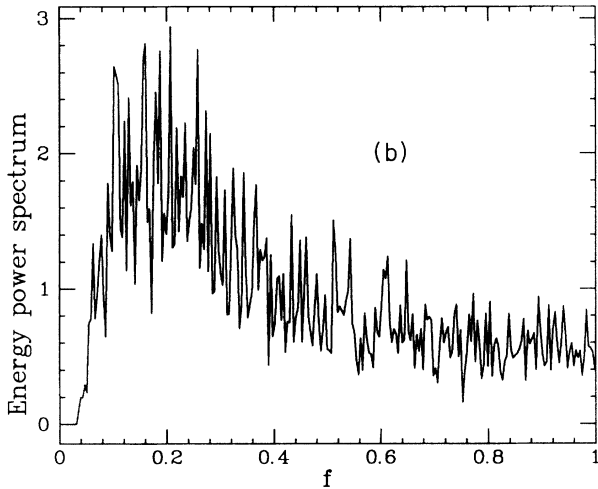
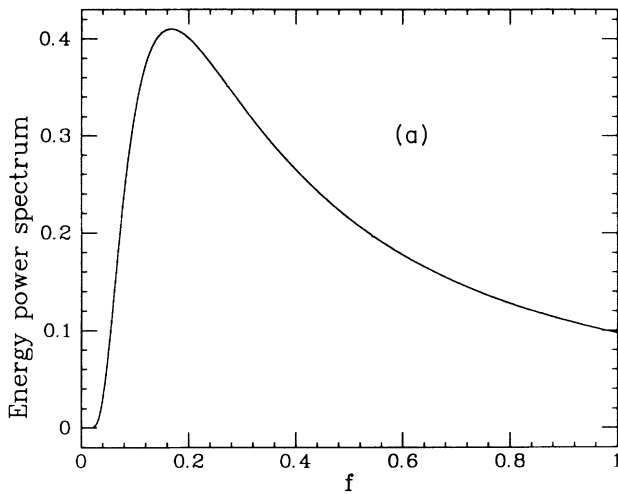


FIG. 2. Comparison between (a): the analytical expression of the first-harmonic energy power spectrum $B_1(f)$, and (b) the power spectrum of $\Delta\varepsilon_n \equiv \varepsilon_n(\phi/\phi_0=0) - \varepsilon_n(\phi/\phi_0=\frac{1}{2})$ calculated numerically in Ref. 13 using the Anderson model on a cylinder $128 \times 10 \times 10$ and $W/t=3$. Note in both cases the low-frequency cutoff, corresponding to $f \ll \Delta/E_c$, and the high-frequency power-law tail. Energy power spectrum is in arbitrary units.

and is found to be

$$\langle I_m^2 \rangle = \frac{24s^2 E_c^2}{m^3 \phi_0^2}, \quad (3.13)$$

in agreement with the results of Ref. (26) for the current harmonics in a SNS junction (see also Ref. 19).

To conclude this section, we compare our results to the numerical study of Refs. 12 and 13. The quantity evaluated there was the power spectrum of

$$\Delta\varepsilon_n \equiv \varepsilon_n \left[\frac{\phi}{\phi_0} = 0 \right] - \varepsilon_n \left[\frac{\phi}{\phi_0} = \frac{1}{2} \right], \quad (3.14)$$

where the index n runs over levels. This quantity may be represented as a sum over the odd harmonics $(2m+1)$ of $\varepsilon_n(\phi/\phi_0)$, cf. Eq. (2.5):

$$\Delta\varepsilon_n = 2 \sum_m \lambda_{2m+1}^{(n)}. \quad (3.15)$$

By Eq. (2.7), and using the fact that upon ensemble averaging different harmonics are uncorrelated [cf. Eq. (3.7)], the power spectrum $\langle [\Delta\varepsilon(f)]^2 \rangle$ is given by

$$\langle [\Delta\varepsilon(f)]^2 \rangle = \sum_m B_{2m+1}(f). \quad (3.16)$$

Considering $f \gg \Delta/E_c \approx 1/M_{\text{eff}}$, we may use for B the analytic expression, Eq. (3.1), and replace the discrete sum in Eq. (3.16) by an integral. The power spectrum then reads

$$\langle [\Delta\varepsilon(f)]^2 \rangle = \frac{\Delta^2}{(M_{\text{eff}})^{1/2}} f^{3/2} \int_0^\infty e^{-f_m/f} dm \sim \frac{\Delta^2}{f}. \quad (3.17)$$

In the low- f limit, $fM_{\text{eff}} \ll 1$,

$$\langle [\Delta\varepsilon(f)]^2 \rangle \sim B_1(f) \approx 0. \quad (3.18)$$

We have thus recovered the $1/f$ high-“frequency” tail of the “power spectrum” found numerically, as well as the low- f vanishing of the “power spectrum,” reflecting the spectral rigidity over large energies.

IV. CORRELATION OF THE LEVEL CURVATURES

A. Hollow cylinders

Single-level current-current correlations are easily derived from Eq. (2.19) by taking the appropriate derivatives with respect to ϕ_1 and ϕ_2 . In order to facilitate comparison with correlation functions of simply connected geometries, it is useful to write down these correlation functions in a compact form, summing over the Fourier components that appear in Eq. (2.19) (cf. Ref. 20).

Employing Eqs. (2.16), (2.17), and (2.19), we obtain the single-level curvature-curvature correlation function. Denoting the relevant energy interval $\delta = (n-m)\Delta$, we obtain

$$C_{\text{AB}}(\delta) = \lim_{\phi_1, \phi_2 \rightarrow 0} \left\langle \left[-\frac{\partial^2 \varepsilon_n(\phi_1)}{\partial \phi_1^2} \right] \left[-\frac{\partial^2 \varepsilon_m(\phi_2)}{\partial \phi_2^2} \right] \right\rangle, \quad (4.1)$$

where AB denotes Aharonov-Bohm geometry,

$$C_{AB}(\delta) = a \operatorname{Re} \left[\frac{2}{\left[\sinh \frac{z}{2} \right]^2} + \frac{3}{\left[\sinh \frac{z}{2} \right]^4} \right], \quad (4.2)$$

with

$$z = \left[\frac{\gamma - i\delta}{E_c} \right]^{1/2} \quad (4.3)$$

and

$$a = 4s^2 \pi^2 \frac{\Delta^2}{\phi_0^4}. \quad (4.4)$$

In the limit $\delta, \gamma \ll E_c$,

$$C_{AB}(\delta) = 48a \frac{(\gamma^2 - \delta^2) E_c^2}{(\gamma^2 + \delta^2)^2}, \quad (4.5)$$

$C_{AB}(\delta)$ is negative for $\delta > \gamma$. This result implies that the zero-flux curvatures of consecutive energy levels tend to be anticorrelated. On the other hand, in the limit where $\Delta < \gamma, E_c \ll \delta$,

$$\begin{aligned} C_{AB}(\delta) &= 8a \exp \left[- \left(\frac{\delta}{2E_c} \right)^{1/2} \right] \cos \left[\frac{\delta}{2E_c} \right]^{1/2} \\ &= 8a F \left[\frac{\delta}{E_c} \right] \end{aligned} \quad (4.6)$$

[cf. Eq. (2.20)]. In this limit it is the first harmonic of the energy-level correlation function [cf. Eq. 2.19] which contributes to $C_{AB}(\delta)$.

B. Comparison with simply connected geometries

It is interesting to compare the above calculations with the corresponding correlation functions calculated for simply connected geometries. Evidently there is no Aharonov-Bohm flux periodicity to consider. Instead, we study the correlations between the zero-flux curvatures of single electron levels (referred to as ‘‘curvature-curvature correlations’’).

For convenience, and in order to facilitate comparison between correlations over large energy intervals ($\delta \gg E_c$) and small energy intervals ($\delta \ll E_c$), we consider here an anisotropic rectangular box of linear dimensions L_x, L_y , and L_z , as shown in Fig. 3. There is a magnetic field H in the z direction, with the corresponding vector potential

$$\mathbf{A}(0, -Hx, 0). \quad (4.7)$$

We evaluate the following correlation function (the subscript SC stands for simply connected):

$$C_{SC}(\delta) \equiv \lim_{H_1, H_2 \rightarrow 0} \left\langle \left[- \frac{\partial^2 \varepsilon_n(H_1)}{\partial H_1^2} \right] \left[- \frac{\partial^2 \varepsilon_m(H_2)}{\partial H_2^2} \right] \right\rangle. \quad (4.8)$$

Technically speaking, we consider the H^2 corrections

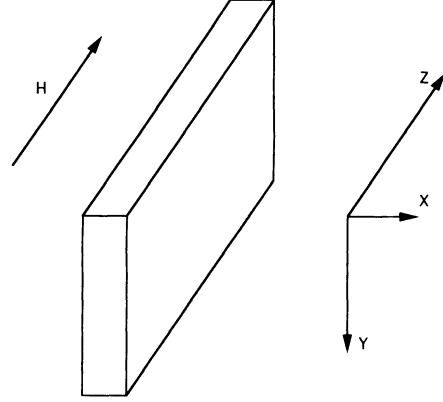


FIG. 3. An anisotropic rectangular geometry with a perpendicular magnetic field.

of the diffusion and cooperon contributions to $C_{SC}(\delta)$. The z modes of the cooperon (or diffuson) are unaffected by the presence of weak field directed along the z axis. For $L_x \ll L_y$ one is left with magnetic-field corrections that depend only on the quantum number of the x mode [the dependence of the $O(H^2)$ correction on the quantum number of the y mode is down by a factor of $(L_x/L_y)^2$]. If we further assume

$$E_{c_x} \equiv \frac{\hbar D}{L_x^2} \gg \gamma, \quad (4.9)$$

γ being the relevant inelastic broadening, we may include only the zeroth mode in the x direction (that is, replace Dq_x^2 in the diffuson pole by 0, cf. Refs. 6 and 20).

We are now in a position to treat various scenarios, depending on the inequalities among γ , $E_{c_y} \equiv \hbar D/L_y^2$, $E_{c_z} \equiv \hbar D/L_z^2$ and δ . To make our point, it is sufficient to restrict ourselves to one specific case, e.g., $L_y \gg L_z$, and

$$E_{c_x}, E_{c_z} \gg \gamma. \quad (4.10)$$

One may easily extend and modify the present treatment to include other inequalities. In evaluating the diffuson and cooperon contributions to the correlation function, Eq. (4.8), we may now sum over the y modes, considering the zeroth modes only in both the x and z directions. Under these assumptions it is possible to account for the weak magnetic-field shift of the relevant cooperon (diffuson) eigenvalues by considering the shift of the zeroth mode (i.e., the product of the zeroth modes in the x, y , and z directions). This shift for the cooperon (diffuson) is $\alpha(H_1 + H_2)^2 [\alpha(H_1 - H_2)^2]$. We obtain

$$\begin{aligned} C_{SC} &= \frac{6s^2}{\pi^2 E_{c_y}^2} \alpha^2 \operatorname{Re} \left[\frac{1}{z^2 \sinh^2 z} + \frac{1}{z^3 \tanh z} \right], \\ z &= \left[\frac{\gamma - i\delta}{E_{c_y}} \right]^{1/2}. \end{aligned} \quad (4.11)$$

Let us now discuss the following limiting cases:

(i) $\Delta \ll \gamma$, $\delta \ll E_{c_y}$. Straightforward evaluation of the correlation function yields

$$C_{\text{SC}}(\delta) = \frac{12s^2}{\pi^2\Delta^2} \alpha^2 \frac{\gamma^2 - \delta^2}{(\gamma^2 + \delta^2)^2}. \quad (4.12)$$

It should be noted that an identical expression (but with a different value for α) is obtained for a simply connected, cylindrically shaped system (with the field oriented along the cylinder's axis). In this weak-field small-energy interval regime this expression is also equal—up to a geometrical factor—to the corresponding correlation function calculated for an Aharonov-Bohm cylinder. We note that for $\delta > \gamma > \Delta$ level curvatures tend to be anticorrelated, providing an explanation for the weak-field anomalous paramagnetic behavior of mesoscopic conductors (cf. Refs. 15, 20, and 25).

(ii) $\gamma \ll E_{c_y} \ll \delta \ll E_{c_x}$. We obtain

$$C_{\text{SC}}(\delta) = -\frac{3\sqrt{2}}{\pi^2\Delta^2} \frac{\alpha^2}{(E_{c_y})^2} \left(\frac{E_{c_y}}{\delta} \right)^{3/2}. \quad (4.13)$$

For $E_{c_x} \ll \delta \ll E_{c_x}$ we expect a different power-law behavior. This monotonic power-law decay of the correlations comes in sharp contrast with the exponentially attenuated oscillations, found in the case of an Aharonov-Bohm system [cf. Eq. (4.6) and Fig. 4]. This difference is a direct consequence of the fact that a *typical* diffusing trajectory which is flux sensitive (i.e., winds around the cylinder at least once) is associated with long times ($> \hbar/E_c$), i.e., small energies. For large energy intervals the distinction between simply connected geometries and

multiply connected ones becomes apparent. This is also responsible for the fact that the average susceptibility, say, is suppressed exponentially with the inelastic rate (or temperature) in the case of a hollow cylinder^{14–17} (for temperatures larger than E_c), while it is attenuated as a power law for simply connected systems.^{20,25}

There are other limiting cases that may be discussed here. For example, for E_{c_y} , $\delta \ll \gamma$ (macroscopic regime) one obtains again a power-law decay

$$C_{\text{SC}} = \frac{6s^2}{\pi^2\Delta^2} \frac{\alpha^2}{(E_{c_y})^2} \left(\frac{E_{c_y}}{\gamma} \right)^{3/2}. \quad (4.14)$$

The inelastic broadening γ gives rise to contributions from the correlation of a level with itself, deeming the correlation function positive.

The above analysis demonstrates that the flux-dependent part of the spectrum is much less rigid on large energy scales in the case of simply connected systems than it is for an Aharonov-Bohm flux. For the latter we have shown how it is possible to evaluate the averaged square current (the total typical current) or, for this purpose, the total typical susceptibility,^{26–29} by double integrating over single-level contributions up to the Fermi energy. In principle this procedure could be repeated when considering a simply connected system. But in that case, and due to the lesser rigidity of the spectrum, it is crucial to account for correlations over distances larger than \hbar/τ . The introduction of a cutoff $W \leq \hbar/\tau$ in the energy integrations involved is, at the present case, not quite satisfactory.

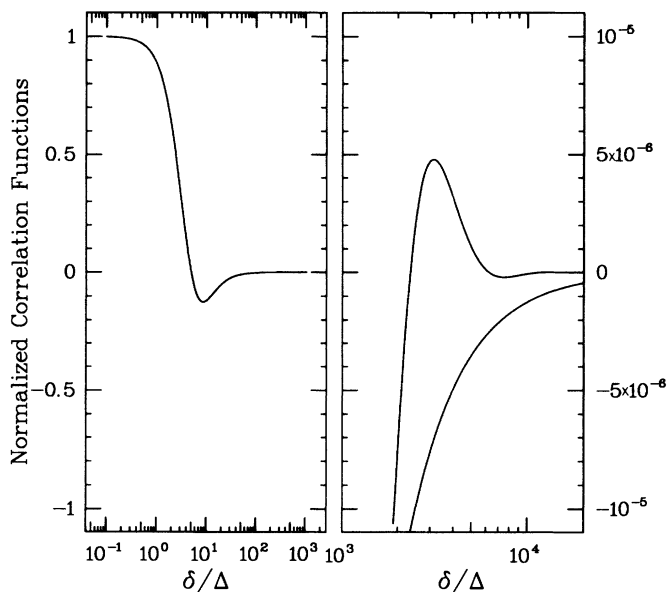


FIG. 4. Comparison between the correlation function of the level curvatures for the cylinder and the quantum dot, normalized at 1 for $\delta=0$. The parameters are $E_c = E_{c_y} = 50\Delta$ and $\gamma = 5\Delta$. Note that these functions are identical in the low-energy limit $\delta < E_c$ but strongly differ in the large-energy limit $\delta \gg E_c$. The upper curve corresponds to the case of the cylinder, the lower curve corresponds to the case of the rectangular quantum dot.

V. SUMMARY AND DISCUSSION

We have revisited some of the outstanding issues in the study of magnetic-field-dependent, noninteracting mesoscopic systems. It is convenient to express various quantities of interest in terms of the single-electron-level correlations. In particular, we have analyzed the flux-dependent part of these correlations in Aharonov-Bohm cylinders, and compared them with the related correlations in simply connected systems subject to weak magnetic fields.

For Aharonov-Bohm geometries, the correlation function is periodic in the flux. Any given harmonic is energy dependent, and fluctuates as function of energy. On large energy scales the correlation function of the m th harmonic in the energy direction consists of exponentially attenuated oscillations of the variable $m\sqrt{\delta/E_c}$, where δ is the energy difference at hand and E_c is the Thouless energy. The fact that the typical value of the total current is proportional to E_c , and is independent of the total number of electrons in the ring, is a direct consequence of the rigidity of the flux-dependent spectral correlations on large energy scales (and is directly associated with the fact that the correlation function in the energy direction falls off stretched exponentially rather than exponentially). The rigidity is also reflected in the analysis of the “power spectrum” of the single-level currents.

In contrast, for simply connected systems, the large energy correlation falls off power law, exhibiting no oscillations.

tions. The difference between the two geometries can be traced back to the fact that for energies larger than E_c (corresponding to time scales shorter than the transversal time across the system), only an exponentially small fraction of the electron's semiclassical trajectories will go at least once around the Aharonov-Bohm cylinder, giving rise to flux sensitivity. In contrast, for simply connected geometries, even relatively short trajectories may be flux (or field) sensitive.

On smaller energy scales ($\delta \ll E_c$) the correlation functions are similar for hollow cylinders and simply connected geometries. The curvature-curvature correlation function is negative for $\delta > \Delta$, corroborating the fact that subsequent levels tend to be anticorrelated in their curvature, in agreement with the Bouchiat-Montambaux picture.

We note that throughout this work we have not accounted in detail for correlations over energy scales

larger than \hbar/τ . This, of course, require further justification.²³ For this purpose, the existence of certain sum rules that govern the spectral rigidity over large energy scales may be essential.

ACKNOWLEDGMENTS

We acknowledge useful discussions with and elaborating comments from A. Altland, B. L. Altshuler, Y. Imry, L. Levy, and G. Montambaux. This research was supported in part by the German-Israel Foundation (GIF) and by the U.S.-Israel Binational Science Foundation (BSF), Jerusalem. Y.G. is thankful to H.B. and G. Montambaux for their hospitality during his visits to Laboratoire de Physique des Solides, Orsay, where parts of this work have been performed. Laboratoire de Physique des Solides is associé au Centre National de la Recherche Scientifique.

-
- ¹L. P. Lévy, G. Dolan, J. Dunsmuir, and H. Bouchiat, *Phys. Rev. Lett.* **64**, 2074 (1990).
²L. P. Lévy, *Physica B* **169**, 245 (1991).
³H. Bouchiat, G. Montambaux, L. Lévy, G. Dolan, and J. Dunsmuir, in *Quantum Coherence in Mesoscopic Systems*, edited by B. Kramer (Plenum, New York, 1991), p. 245.
⁴Y. Imry, *Nature*, **345**, 574 (1990).
⁵V. Chandrasekhar, R. A. Webb, M. J. Brady, M. B. Ketchen, W. J. Gallagher, and A. Kleinsasser, *Phys. Rev. Lett.* **67**, 3578 (1991).
⁶B. L. Altshuler and B. I. Shklovskii, *Zh. Eksp. Teor. Fiz.* **91**, 220 (1986) [*Sov. Phys. JETP* **64**, 127 (1986)].
⁷Y. Imry, in *Quantum Coherence in Mesoscopic Systems* (Ref. 3), p. 221.
⁸H. F. Cheung, E. K. Riedel, and Y. Gefen, *Phys. Rev. Lett.* **62**, 587 (1989).
⁹N. Argaman, Y. Imry, and U. Smilansky (unpublished).
¹⁰H. F. Cheung, Y. Gefen, E. K. Riedel, and W. H. Shih, *Phys. Rev. B* **37**, 6050 (1988).
¹¹H. Bouchiat and G. Montambaux, *J. (Paris)* **50**, 2695 (1989).
¹²G. Montambaux, H. Bouchiat, D. Sigeti, and R. Friesner, *Phys. Rev. B* **42**, 7647 (1990).
¹³H. Bouchiat, G. Montambaux, and D. Sigeti, *Phys. Rev. B* **44**, 1682 (1991).
¹⁴A. Schmid, *Phys. Rev. Lett.* **66**, 80 (1991).
¹⁵B. L. Altshuler, Y. Gefen, and Y. Imry, *Phys. Rev. Lett.* **66**, 88 (1991).
¹⁶F. von Oppen and E. K. Riedel, *Phys. Rev. Lett.* **66**, 8 (1991).
¹⁷E. A. Ackermans, *Europhys. Lett.* **15**, 709 (1991).
¹⁸A. Altland, A. Müller-Groeling, S. Iida, and H. A. Weidenmüller, *Europhys. Lett.* **20**, 155 (1992); *Ann. Phys.* (to be published).
¹⁹E. K. Riedel and F. von Oppen, *Superlatt. Microstruct.* **11**, 179 (1992).
²⁰S. Oh, A. Yu. Zyuzin, and R. A. Serota, *Phys. Rev. B* **44**, 8858 (1991).
²¹Y. Imry, in the *Proceedings of the 1991 Taniguchi Symposium on Mesoscopic Physics*, edited by H. Fukuyama and T. Ando (Springer, Berlin, 1992).
²²D. de Vincenzo and M. P. A. Fisher (unpublished).
²³A. Altland and Y. Gefen (unpublished).
²⁴K. B. Efetov, *Phys. Rev. Lett.* **66**, 2794 (1991).
²⁵B. L. Altshuler, Y. Gefen, Y. Imry, and G. Montambaux (unpublished).
²⁶O. D. Cheishvili, *Pis'ma Zh. Eksp. Teor. Fiz.* **48**, 206 (1988) [*JETP Lett.* **48**, 2225 (1988)].
²⁷H. Fukuyama, *J. Phys. Soc. Jpn.* **58**, 47 (1989).
²⁸E. Ackermans and B. Shapiro, *Europhys. Lett.* **11**, 467 (1990).
²⁹R. A. Serota and S. Oh, *Phys. Rev. B* **41**, 10 523 (1990).